

THE STARBURST NATURE OF LYMAN-BREAK GALAXIES: TESTING UV EXTINCTION WITH X-RAYS

MARK SEIBERT, TIMOTHY M. HECKMAN AND GERHARDT R. MEURER

The Johns Hopkins University, Department of Physics and Astronomy
3400 North Charles Street, Baltimore, MD 21218
mseibert@pha.jhu.edu, heckman@pha.jhu.edu, meurer@pha.jhu.edu

Accepted for publication in the Astronomical Journal

ABSTRACT

We derive the bolometric to X-ray correlation for a local sample of normal and starburst galaxies and use it, in combination with several UV reddening schemes, to predict the 2–8 keV X-ray luminosity for a sample of 24 Lyman-break galaxies in the HDF/CDF-N. We find that the mean X-ray luminosity, as predicted from the Meurer UV reddening relation for starburst galaxies, agrees extremely well with the Brandt *stacking* analysis. This provides additional evidence that Lyman-break galaxies can be considered as scaled-up local starbursts and that the locally derived starburst UV reddening relation may be a reasonable tool for estimating the UV extinction at high redshift. Our analysis shows that the Lyman-break sample can not have far-IR to far-UV flux ratios similar to nearby ULIGs, as this would predict a mean X-ray luminosity 100 times larger than observed, as well as far-IR luminosities large enough to be detected in the sub-mm. We calculate the UV reddening expected from the Calzetti effective starburst attenuation curve and the radiative transfer models of Witt & Gordon for low metallicity dust in a shell geometry with homogeneous or clumpy dust distributions and find that all are consistent with the observed X-ray emission. Finally, we show that the mean X-ray luminosity of the sample would be under predicted by a factor of 6 if the the far-UV is unattenuated by dust.

Subject headings: galaxies: high-redshift — galaxies: starburst — ultraviolet: galaxies — X-rays:
galaxies — infrared: galaxies

1. INTRODUCTION

Lyman-break galaxies (LBGs) represent the sites of a significant fraction of the star formation in the early universe (e.g., Adelberger & Steidel 2000) and the ultraviolet (UV) derived star formation rates (SFRs) of LBGs have become an important component of the recent attempts to measure the star formation history of the universe (e.g., Madau et al. 1996; Steidel et al. 1999; Lanzetta et al. 2002). Precisely how the UV emission of LBGs are corrected for the effects of intrinsic dust attenuation, which requires a knowledge about the true nature of these objects, is critical for estimating star formation rate densities at $z > 2$.

Starburst galaxies are the most likely local analogs to the population of LBGs at high redshift. LBGs have UV surface brightnesses and UV colors similar to local starbursts (Meurer et al. 1997) suggesting that LBGs can be considered as larger and more luminous versions of the nearby variety. Further evidence in support of the analogy comes from the only high quality rest-frame UV spectrum of an individual LBG – the gravitationally lensed MS 1512+36-cB58 – which shows emission and absorption features remarkably consistent with local starbursts (Pettini et al. 2000).

Local starburst galaxies exhibit an empirical correlation between their UV spectral slope (β ; equivalent to UV color) and their infrared excess (IRX; ratio of far-IR to far-UV flux). This relationship implies that starbursts redden as dust absorption increases and that dust surrounding starburst regions can be modeled to provide an estimate of the UV extinction as a simple linear function of the UV color (Meurer et al. 1999; hereafter MHC99).

Although the UV properties of LBGs can be readily measured from deep optical imaging, obtaining rest-frame far-IR data for these high redshift galaxies is extraordinarily difficult. Therefore, it is unclear whether or not the IRX- β reddening relationship is a meaningful tool that may be used to estimate the UV extinction of high redshift galaxies. Until rest-frame far-IR data become available for a significant sample of LBGs, we must attempt to probe other accessible wavelength windows that may provide clues about the thermal dust emission. X-rays can be just such a proxy.

In this paper, we investigate the suggested starburst nature of LBGs by considering their X-ray emission and the consequences for UV extinction. To do this, we first use a local sample of normal and starburst galaxies to demonstrate a clear correlation between the bolometric and 2–8 keV X-ray luminosities when the bolometric output is dominated by far-IR and far-UV emission. We then test the starburst concept for LBGs by applying the starburst derived IRX- β relationship to a sample of 24 LBGs in order to predict their X-ray emission. Specifically, we estimate the far-IR luminosity using the starburst UV reddening relationship and then estimate the X-ray luminosity from the bolometric to X-ray correlation. These results are compared to the recent 1 Ms exposure Chandra Deep Field North (CDF-N) X-ray constraints of Brandt et al. (2001) for the same sample.

It is possible that the UV properties of LBGs are only superficially starburst-like. Perhaps they are the UV-bright portion of ‘scaled-up’ ultraluminous infrared galaxies (ULIGs) and the majority of UV light generated by star formation is heavily extinguished and not detected in rest-UV

surveys (e.g., Goldader et al. 2002). Certainly the irregular morphology of LBGs is consistent with the notion that they are recent mergers or interacting systems. Alternatively, LBGs may be youthful proto-galaxies in the process of forming the spheroids destined to become the central bulges of spirals or elliptical galaxies. If so, LBGs could be relatively free from the effects of dust because they have not yet been enriched with a significant quantity of heavy elements. These scenarios represent the extremes of UV extinction in LBGs and, consequently, extremes of their estimated star formation rates (SFRs) as well. We test several alternative hypotheses by adapting our technique to estimate the X-ray luminosities assuming that LBGs 1) have far-UV and far-IR properties consistent with those found by Goldader et al. (2002) for ULIGs, 2) have low metallicity (SMC-type) dust as modeled by Witt & Gordon (2000) or parameterized by the effective attenuation curve for starbursts (Calzetti et al. 2000) or 3) have stellar populations unattenuated by dust.

2. THE LYMAN-BREAK SAMPLE

We adopt the sample of 24 Lyman-break galaxies from the Hubble Deep Field North (HDF-N) survey region within the CDF-N used by Brandt et al. (2001), so that we may compare our X-ray predictions to their X-ray measurements. The sample selection process we follow is described in detail by Brandt et al., and is based upon two criteria; 1) galaxies are spectroscopically confirmed as high redshift with $z = 2-4$ and 2) none is individually detected or are within $\sim 8''$ of a detected source by *Chandra*. The spectroscopic redshifts are compiled from the Caltech Faint Galaxy Redshift Survey (Cohen et al. 2000) and the serendipitous catalog of Dawson et al. (2001). The sample is listed in Table 1. We use the observed-frame optical measurements of the HDF-N catalog (Williams et al. 1996). The mean (median) redshift of the sample is 2.79 (2.93).

3. THE OBSERVED X-RAY EMISSION OF THE LYMAN-BREAK GALAXY SAMPLE

The observed mean X-ray emission for the LBG sample has recently been determined by Brandt et al. (2001) by *stacking* the counts of each galaxy from the 1 Ms CDF-N survey data into an image with an effective exposure time of 260 days (22.4 Ms). They found 43 counts within the 30 pixel aperture of the *stacked* image for the soft (0.5–2 keV observed-frame) bandpass. The expected background counts were 26.2. The statistically significant detection (99.9% confidence level for Poisson statistics) gives an average count rate of 7.5×10^{-7} count s⁻¹. The *Chandra* soft band corresponds to a rest-frame bandpass of 2–8 keV at the median redshift of the sample. The opacity of interstellar gas in this spectral range is comparable to the opacity at $\lambda = 3-60 \mu\text{m}$ (Morrison & McCammon 1983; Draine & Lee 1984). For a neutral interstellar medium with a column density of $N_{\text{H}} = 1.0 \times 10^{21} \text{ cm}^{-2}$ the optical depth at 2 keV ($\tau_{2\text{keV}}$) is only 0.04 (Morrison & McCammon 1983).

Brandt et al. assume an intrinsic power law spectrum with photon index $\Gamma = 2$ (typical of X-ray binaries and low luminosity AGN) and a mean column density for the CDF-N of $N_{\text{H}} = 1.6 \times 10^{20} \text{ cm}^{-2}$ in order to estimate a mean flux of $4.0 \times 10^{-18} \text{ erg s}^{-1} \text{ cm}^{-2}$. The mean ob-

served rest-frame 2–8 keV luminosity is $2.8 \times 10^{41} \text{ erg s}^{-1}$ for $H_0 = 70 \text{ km s}^{-1} \text{ Mpc}^{-1}$ ($\Omega_M = 1/3$, $\Omega_\Lambda = 2/3$) at the sample's median redshift.

We crudely estimate two sources of possible error for the mean flux: 1) 49% random error from photon counting and 2) 30% systematic error due to choice of intrinsic X-ray spectrum. The photon counting error is taken as the quadrature sum of the total count error ($\pm\sqrt{43}$) and the background count error ($\pm\sqrt{26.2}$). The systematic error is assessed by computing the differences in X-ray flux assuming variations in N_{H} and Γ for the power law spectral model as well as alternative Raymond-Smith plasma and thermal bremsstrahlung models. Combining the random and systematic errors in quadrature yields a total error estimate of $\sim 58\%$ ($\log L_{\text{X,obs}} = 41.45 \pm 0.25$).

4. THE LOCAL BOLOMETRIC TO X-RAY CORRELATION

Several authors have published far-IR to X-ray correlations for a wide variety of galaxy types and AGNs (e.g., David et al. 1992; Green et al. 1992; Ranalli et al. 2002). We have adopted the normal and starburst galaxy sample of David et al. (1992) as our starting point for defining the bolometric to X-ray correlation because of the large sample size (71) and the consistent spectral model employed to obtain X-ray fluxes from count rates. The X-ray data used by David et al. are from *Einstein* IPC (0.5–4.5 keV) observations and fluxes are derived assuming the intrinsic emission is given by a $kT = 5 \text{ keV}$ Raymond-Smith plasma with solar abundances and a mean hydrogen column density of $N_{\text{H}} = 10^{20} \text{ cm}^{-2}$. Far-IR fluxes are based on IRAS 60 and 100 μm flux densities as defined by Helou et al. (1988). David et al. computed X-ray and far-IR luminosities for the sample using distances from Sandage & Tammann (1975, 1981) or from the redshifts published by Soifer et al. (1987). We adjust all luminosities to reflect our adopted H_0 .

As our intention is to predict the rest 2–8 keV X-ray luminosity of the Lyman-break sample we apply a correction to the David et al. X-ray flux measurements that will account for the difference in bandpass and intrinsic spectral model. Using the X-ray spectral fitting package XSPEC (Arnaud 1996) we have modeled the spectrum in the 0.5–8 keV range as a power law spectrum with photon index $\Gamma = 2$. The photon count rate in the 0.5–4.5 keV range was normalized to that expected for a 0.5–4.5 keV flux of $5.5 \times 10^{-18} \text{ erg s}^{-1} \text{ cm}^{-2}$ (the mean of the David et al. sample) from a 5 keV Raymond-Smith plasma with solar abundances. Photoelectric absorption was applied using $N_{\text{H}} = 10^{20} \text{ cm}^{-2}$. The result is a correction factor of order unity ($F_{2-8,\text{PL}}/F_{0.5-4.5,\text{RS}} = 0.6$).

We estimate the bolometric output of this star forming galaxy sample by assuming that it is dominated by young stellar populations. This allows us to approximate the bolometric luminosity from the far-IR and far-UV using;

$$L_{\text{Bol}} = L_{\text{FUV}} \times \text{BC}_{\text{stars}} + L_{\text{FIR}} \times \text{BC}_{\text{dust}}, \quad (1)$$

where BC_{dust} is the bolometric correction for the FIR to the 1–1000 μm dust emission and BC_{stars} is the bolometric correction for the far-UV to the 0.0912–1 μm unextincted stellar emission of an active star forming population. We use the value of $\text{BC}_{\text{dust}} = 1.75$ determined by Calzetti et al. (2000) from *ISO* and *IRAS* photometry of a sample of eight low redshift star forming galaxies. We take

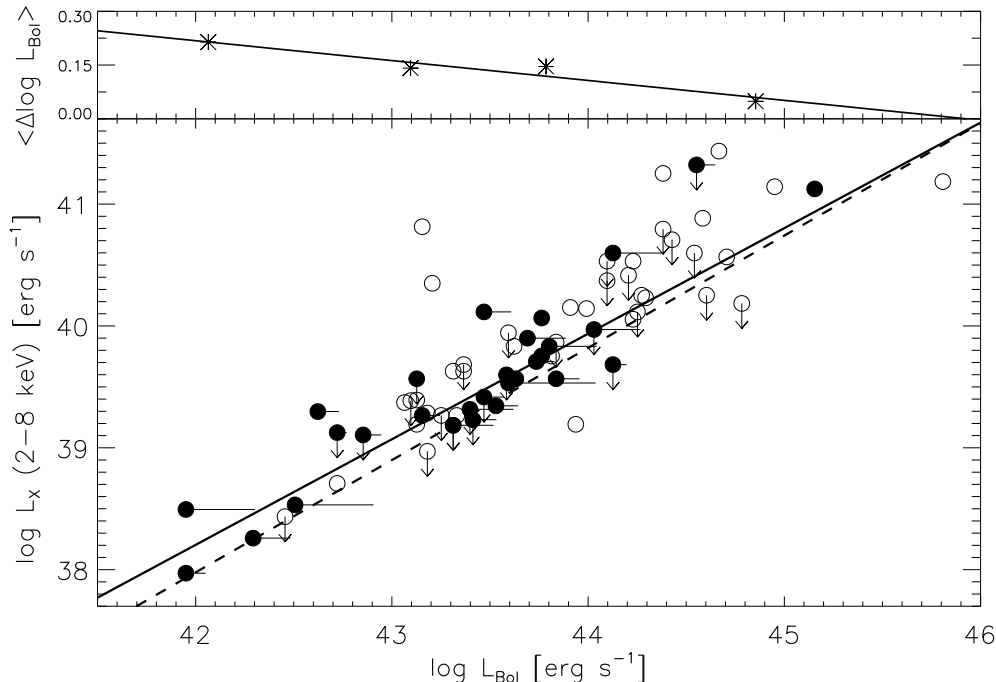


FIG. 1.— BOTTOM: The bolometric to X-ray correlation for normal and starburst galaxies. The sample is from David et al. (1992). The X-ray luminosity is derived from *Einstein* IPC data and corrected for bandpass and spectral model. All circles represent L_{Bol} estimated from the far-IR only ($L_{\text{Bol[FIR]}}$). Solid circles represent a subsample where far-UV data is also available and the effect on L_{Bol} is shown with horizontal lines ($L_{\text{Bol[FIR,FUV]}}$). The solid line is the fit to the entire sample (71) using $L_{\text{Bol[FIR]}}$. The dashed line is the fit to the subsample (29) using $L_{\text{Bol[FIR,FUV]}}$. The fits account for data points with the 3σ X-ray upper limits indicated with downward arrows (see text). TOP: The difference between $\log L_{\text{Bol[FIR,FUV]}}$ and $\log L_{\text{Bol[FIR]}}$ for the subsample. The data has been grouped in bins of 1 dex and the mean difference is plotted against mean $\log L_{\text{Bol[FIR]}}$. The line is a simple chi-square linear fit.

$BC_{\text{stars}} = 1.66$ ($\lambda = 1600\text{\AA}$) computed by MHC99 from a range of Starburst99 synthetic starburst spectra (Leitherer et al. 1999). We have obtained far-UV fluxes for 29 of the 71 galaxies in the sample from either the UV catalog of Marcum et al. (2001) at 1550\AA or the homogenized UV catalog of Rifatto et al. (1995) at 1650\AA .

Of the 71 galaxies in this sample, 28 have 3σ upper limits to the X-ray flux. We account for this fact and compute the fit to the correlation by using the Buckley-James¹ linear regression technique which computes coefficients based on Kaplan-Meier residuals. If we consider only the far-IR emission when approximating the bolometric luminosity ($L_{\text{Bol}} = L_{\text{FIR}} \times BC_{\text{dust}}$) we can use all 71 galaxies to find the fit,

$$\log L_{X(2-8)} = (0.87 \pm 0.08) \log(L_{\text{Bol[FIR]}}) + 1.81, \quad (2)$$

shown by the solid line in the bottom panel of Figure 1. The error is 1σ . If we fit only the 29 with both far-IR and far-UV data (of which 11 have X-ray upper limits) using Equation 1 we compute the fit,

$$\log L_{X(2-8)} = (0.92 \pm 0.10) \log(L_{\text{Bol[FIR,FUV]}}) - 0.72, \quad (3)$$

which is represented by the dashed line in the same figure.

The fit becomes slightly steeper when the UV data are properly considered. This is due to the fact that the far-UV contributes measurably to L_{Bol} in systems with lower far-IR luminosities, but has a negligible effect on L_{Bol} at higher far-IR luminosities. The effect is highlighted in the top panel of figure 1 where we plot the difference \log

$L_{\text{Bol[FIR,FUV]}} - \log L_{\text{Bol[FIR]}}$. The 29 data points have been grouped in bins of 1 dex and the mean difference is plotted against $\log L_{\text{Bol[FIR]}}$. The line is a simple chi-square linear fit. The trend is understood most simply as an extinction effect, where the far-UV extinction is positively correlated with L_{Bol} (Heckman et al. 1998). We use the correlation derived from the far-UV and far-IR (Equation 3) for predicting the LBG X-ray output. It is interesting to note that the mean observed X-ray luminosity of the LBG sample suggests a large mean L_{Bol} ($\approx L_{\text{FIR}}$) of $\sim 10^{12} L_{\odot}$. This is at the high luminosity end of the local starburst population.

5. X-RAY PREDICTIONS

5.1. Case I: Estimating X-rays Assuming Starburst Reddening

The assumption that we can model the far-IR to far-UV flux ratio as a function of UV reddening is the crucial component in our technique of predicting the X-ray emission of the LBG sample. We first consider the empirically derived UV reddening relation of MHC99 ($\text{IRX}-\beta$) for local starbursts.

The UV spectral slope (β) is found from the photometric $V_{606} - I_{814}$ color. We use equation 14 of MHC99 which calibrates the spectroscopically defined β to the $(V_{606} - I_{814})_{\text{AB}}$ color as a function of redshift between $z = 2-4$. The ABmag system colors are from the isophotal

¹ From the Astronomy Survival Analysis (ASURV) task within the STSDAS IRAF package.

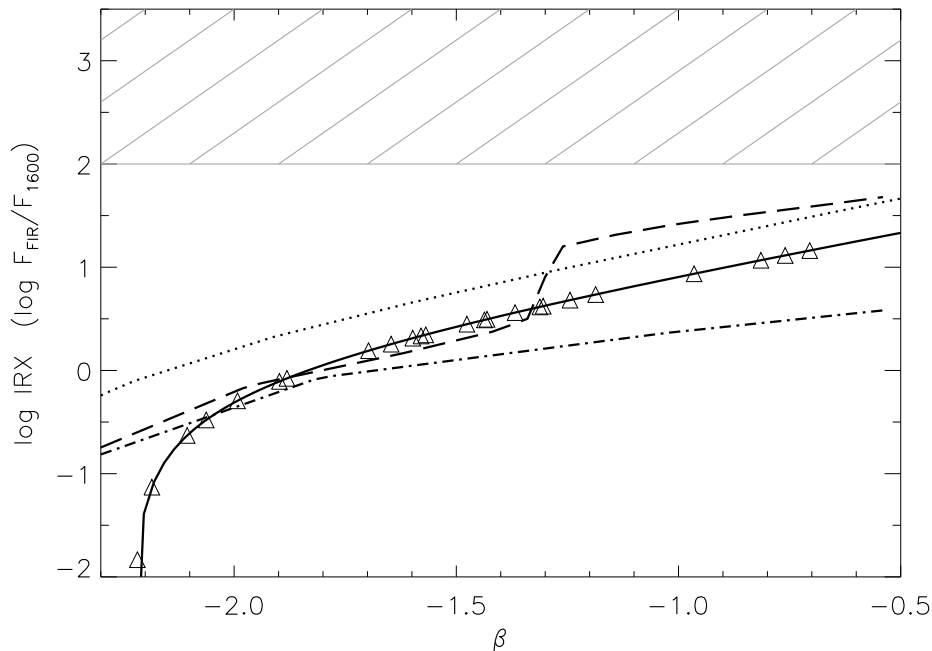


FIG. 2.— UV reddening relationships used to estimate the far-IR of the LBG sample. The solid line is the empirical IRX- β starburst relation of MHC99. Triangles are the LBG sample with IRX derived from the MHC99 relation and photometrically measured β . The dash-dot line is the UV reddening relation computed from Witt & Gordon (2000) extinction models for SMC-dust in a shell geometry with a homogeneous distribution. The dashed line represents a clumpy dust distribution. The dotted line is based on the Calzetti (2000) mean starburst attenuation curve. The hash marks indicate the region of the IRX- β diagram where objects with ULIG-like UV extinction properties would be located (Goldader et al. 2002).

fluxes in the HDF-N catalog of Williams et al. (1996) corrected for Galactic extinction. The IRX- β reddening relation is then used to predict the far-IR to far-UV flux ratio using the approximation,

$$\text{IRX} \equiv \frac{F_{\text{FIR}}}{F_{1600}} \approx (10^{0.4A_{1600}} - 1) \times \frac{\text{BC}_{\text{stars}}}{\text{BC}_{\text{dust}}}. \quad (4)$$

MHC99 demonstrated that, for starbursts, this is a reasonable estimate for IRX and the extinction term is a simple linear function of β ($A_{1600} = 4.43 + 1.99\beta$).

The form of the MHC99 IRX- β relation can be seen as the solid line in Figure 2. We estimate F_{1600} by interpolating the HDF rest-frame UV data. Equation 4 allows a prediction of the far-IR flux under the assumption that the LBG sample has UV extinction and reddening properties similar to local starbursts. The far-IR and far-UV fluxes are converted to luminosities using the spectroscopically derived redshifts. Finally, we predict the 2–8 keV X-ray luminosities for each Lyman-break galaxy from the bolometric to X-ray correlation.

The 1σ error of the predicted mean is assessed with Monte Carlo error analysis by generating 150 synthetic data sets (3600 total data points). In addition to incorporating the measurement errors of the HDF-N catalog into the synthetic data, the dispersion of the IRX- β (0.25 dex in log IRX) and bolometric to X-ray correlations (0.4 dex in log L_X) are also included. The mean of each synthetic data set is measured and the 1σ error (in dex) is taken as the standard deviation of the distribution of differences

from the true sample mean using

$$\text{Error} = \left(\frac{1}{N} \sum_{i=1}^N (\log \overline{L_{X,t}} - \log \overline{L_{X,i}})^2 \right)^{1/2}, \quad (5)$$

where the subscripts t and i indicate the true LBG sample and i th synthetic data set respectively.

The results are expressed as a histogram of the predicted X-ray luminosities in Figure 3 (Panel A). The log of the mean *linear* luminosity is shown as a solid line with error bars. For comparison, the mean observed value of Brandt et al. is represented as a dashed line. The mean predicted X-ray emission is $2.4 \times 10^{41} \text{ erg s}^{-1}$. This agrees well with the mean observed value. The 1σ error is 0.22 dex. Under this scenario, all of the LBGs in the sample are predicted to have fluxes below the single source soft-band flux limit ($3.0 \times 10^{-17} \text{ erg s}^{-1} \text{ cm}^{-2}$) for the CDF-N (Brandt et al. 2001b).

5.2. Case II: Estimating X-rays Assuming ULIG Properties

Ultraluminous infrared galaxies (ULIGs) do not obey the the IRX- β reddening relation (Goldader et al. 2002). Instead, they occupy a distinct range of log IRX values between ~ 2 –4. Using high resolution *HST* imaging data, Goldader et al. argue that the lack of a significant IRX- β correlation results from the fact that the majority of far-UV light detected from ULIGs originates from the least extinguished sources (possibly just the outermost regions of star formation) and is not coincident with the dust-enshrouded starburst activity responsible for the far-IR emission.

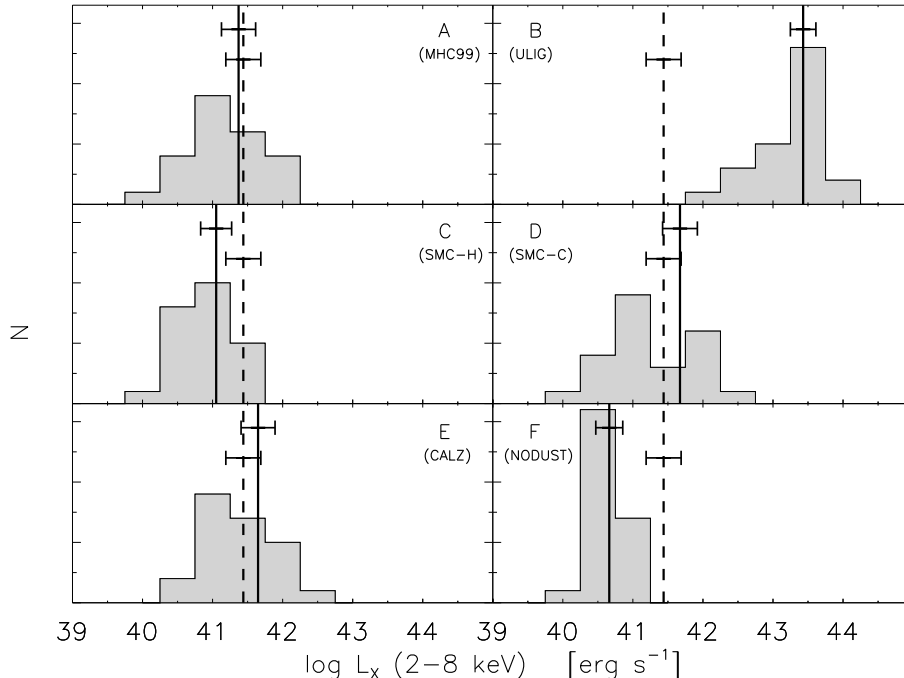


FIG. 3.— Histograms of predicted 2–8 keV X-ray luminosities for the LBG sample. The solid line is the mean of the distribution with Monte Carlo 1σ errors. The dashed line is the observed mean value from Brandt et al. (2001). [A] Assumes the sample obeys the MHC99 IRX- β reddening relationship for starbursts. [B] Assumes UV extinction properties similar to ULIGs. [C] Assumes UV extinction properties consistent with SMC-type dust extinction in a shell geometry with a homogeneous dust distribution. [D] Same as panel C but with a clumpy dust distribution. [E] Assumes UV extinction consistent with the Calzetti starburst effective attenuation curve. [F] Assumes the sample is unattenuated by dust.

To test the likelihood of LBGs being similar to these type of extremely dusty starbursts, we randomly assigned log IRX values in the 2–3.5 range to each LBG (hashed region of Figure 2) and followed the same aforementioned procedure to predict the X-ray luminosities. Our method predicts the mean X-ray luminosity for the sample to be $2.7 \times 10^{43} \text{ erg s}^{-1}$ (Figure 3: Panel B). This is two orders of magnitude larger than the observed value and strongly suggests that LBGs are not hiding a significant amount of star formation behind a veil of dust. In fact, $\sim 92\%$ of the sample would have X-ray fluxes greater than the single source soft-band detection limit, with half being at least an order of magnitude larger.

Furthermore, if LBGs truly have ULIG-like IRX values then the observed far-UV fluxes imply FIR luminosities in the $10^{12.4} - 10^{14.7} L_{\odot}$ range. Using the method described by Adelberger & Steidel (2000) we estimate that 96% of the sample would have rest-frame $\lambda = 200 \mu\text{m}$ flux densities greater than the 2 mJy detection limit for the HDF-N sub-millimeter (sub-mm) survey conducted by Hughes et al. (1998). LBGs, however, have so far proven to be elusive to sub-mm observers (Blain et al. 2002; Chapman et al. 2000; Hughes et al. 1998). The recent sub-mm *stacked* analysis of LBGs by Webb et al. (2002) provides a mean sub-mm 2σ detection of only 0.414 mJy.

5.3. Case III: Estimating X-rays Assuming SMC-type Dust

If LBGs consist of early generation stellar populations, then low metallicity (SMC-type) dust may be appropriate for modeling their global far-IR emission. This would

be consistent with the metallicity of the lensed LBG MS 1512+36-cB58 ($Z \sim 1/4Z_{\odot}$) as constrained by Pettini et al. (2000). We test this idea is with the radiative transfer dust models of Witt & Gordon (2000). We compute the expected IRX and UV spectral slope from Starburst99 (Leitherer et al. 1999) synthetic starburst spectrum after applying extinction effects based on two Witt & Gordon models for SMC-dust in a shell geometry. The first model assumes a homogeneous dust distribution in the surrounding dust shell while the second involves a non-homogeneous ‘clumpy’ distribution.

The adopted Starburst99 spectrum is chosen to be consistent with the low metallicity assumption. It is parameterized by a continuous star formation rate, a Salpeter IMF with slope $\alpha = -2.35$, an upper mass limit of $100 M_{\odot}$, metallicity of $Z = 0.004$, and a burst age of 100 Myr. The bolometric dust luminosity is computed as the sum of the energy from extinguished non-ionizing photons plus the energy deposited from *all* Ly α photons. We estimate the Ly α production, prior to any extinction, by assuming that each ionizing photon generates one Ly α photon (Osterbrock 1989). The luminosity in the FIR bandpass is estimated with BC_{dust} .

The resulting UV reddening relation for the homogeneous dust model is similar in shape to the IRX- β relation of MHC99, but has a slightly less steep slope and is offset to lower values of IRX for a values of $\beta > -2$ (dot-dash line of Figure 2). The UV reddening relation from the alternative clumpy dust distribution is also qualitatively similar to MHC99 but, compared to the homogeneous model, rises faster in IRX before it turns over near $\beta \approx -1.2$ and ob-

tains a similar shallow slope (dashed line in Figure 2). For LBGs in our sample with $\beta > -1.2$, the clumpy model predicts larger values of IRX than the IRX- β relation of MHC99.

Having defined the UV reddening relation expected for the dust models, we again use the same technique to predict the X-ray luminosities of the LBG sample. The homogeneous model slightly under predicts the mean X-ray luminosity (1.1×10^{41} erg s $^{-1}$) compared to the observed value. Within strict error limits (model and observed) the homogeneous model agrees with the observation. The clumpy model slightly over predicts it (4.7×10^{41} erg s $^{-1}$), but the observed mean is well within the 1σ error. The histogram in Panel C (Panel D) of Figure 3 represents the homogeneous (clumpy) model. To within the uncertainties in our technique, we are unable to differentiate between the empirically derived relation of MHC99 and either of the SMC-dust/shell geometry models.

Witt & Gordon claim that the clumpy model reproduces the effective starburst attenuation curve of Calzetti (1997; Calzetti et al. 2000). We have calculated the UV reddening relation for the Calzetti attenuation curve (dotted line of Figure 2) using the same method and find it very similar to the clumpy model over the narrow range of β measured for the LBGs. When we use the Calzetti effective attenuation to predict X-ray emission, we find the mean luminosity (4.5×10^{41} erg s $^{-1}$) is essentially the same as that from the clumpy model and also in agreement with the observed value (Figure 3: Panel E).

We should note the effect our choice of intrinsic starburst model has on the computed UV reddening relations. Choosing a higher metallicity (i.e. Z_{\odot}) stellar population will produce a redder intrinsic (unextincted) spectral slope ($\Delta\beta_0 \sim 0.1$) but would have little effect on IRX values for $\beta > -2$. Differences in either burst age or the IMF upper mass limit will effect both β_0 and IRX in the sense that older bursts or smaller upper mass limits will redden β_0 and lower IRX. This would then result in a smaller predicted X-ray flux for the LBG sample.

5.4. Case IV: Estimating X-rays Assuming No Dust Extinction

We can use the machinery we have developed to test the extreme hypothesis that LBGs suffer no far-UV extinction. If the LBG sample is actively forming stars and harbors little or no dust, we can reasonably assume that the far-UV flux is unattenuated and dominates the bolometric luminosity. The reddened UV colors must then be interpreted as a simple effect of burst age. Although continuous star formation modes could not easily account for the range of β measured in the LBG sample, instantaneous burst modes with ages between $30 > t_{\text{burst}} > 100$ Myr can naturally redden enough to explain the observed UV properties (Leitherer et al. 1999). However, under this scenario, the mean X-ray luminosity is under predicted by a factor of 6 (4.6×10^{40} erg s $^{-1}$). Given the large observational and model uncertainties the difference is $\sim 2\sigma$ (Figure 3: Panel F).

6. CONCLUSIONS

Evidence is beginning to emerge that 2–8 keV X-rays are a good star formation rate indicator (Ranalli et al.

2002). In local starbursts, the 2–8 keV X-ray emission is believed to be produced primarily by high-mass X-ray binaries (HMXB; Persic & Rephaeli 2002). This suggests that the Brandt et al. (2001) stacking technique applied to the HDF-N LBG sample may be detecting binary stars at $z \sim 3$. Low luminosity AGN and the class of ultraluminous X-ray sources (ULXs or IXOs; Colbert & Mushotzky 1999), which may be the beamed emission from HMXBs (i.e., Roberts et al. 2002) or a new class of intermediate mass (10^2 – $10^4 M_{\odot}$) black holes, may also contribute to the 2–8 keV flux. Furthermore, 2–8 keV X-rays suffer little intrinsic absorption and can escape regions where the far-UV tracers of star formation may be heavily extinguished by a dusty interstellar medium. For these reasons, the 2–8 keV X-ray luminosity strongly correlates with the bolometric luminosity of star forming galaxies. This means that 2–8 keV X-rays can serve as a proxy for the far-IR thermal dust emission at high- z .

We have derived the bolometric to 2–8 keV X-ray correlation for a local sample of normal and starburst galaxies and have used it, in combination with several UV reddening schemes, to predict the mean 2–8 keV X-ray luminosity for a sample of 24 spectroscopically confirmed high redshift Lyman-break galaxies. This simple analysis demonstrates that LBGs can not have far-IR to far-UV flux ratios similar to those found for nearby ULIGs, nor are they likely to be unattenuated by dust. Of the extinction methods considered, we find that the IRX- β starburst reddening relation of MHC99 is the most accurate predictor of the mean X-ray luminosity for the sample. The very similar reddening relations derived from Witt & Gordon (2000) extinction models of low metallicity dust in a shell geometry and the Calzetti et al. (2000) effective starburst attenuation curve are also consistent with the observed X-ray emission.

These results provide additional evidence that LBGs can be considered as scaled-up local starbursts. Equally important, it suggests that IRX- β may be a reasonable tool for estimating the UV extinction of high redshift LBGs. If this is the case, all 24 LBGs in this sample have $A_{1600} < 3.1$ Mag with a mean (median) of 1.4 (1.5) Mag implying a mean 1600Å dust correction factor of ~ 4 . This moderate level of UV extinction is consistent with the results of Papovich et al. (2001) who find typical 1700Å correction factors of 3–4.4 from an analysis of the UV-optical spectral energy distributions for a sample of 33 HDF-N LBGs which includes 23 from our sample. Similar UV extinctions are also deduced for larger LBG samples by Steidel et al. (1999) and MHC99. Our results are the first to use low extinction X-ray emission to test and confirm these claims.

Although it is tempting to use the results developed here to predict the X-ray fluxes of individual LBGs, we caution the reader that our results are statistical. The accuracy of the estimated X-ray emission for any single LBG in this sample is only ~ 0.48 dex. With this in mind, it is interesting to note that when the UV reddening relations of MHC99, Witt & Gordon (clumpy model), and Calzetti are applied to this technique, more than 80% of the 2–8 keV flux originates from the half of the sample (12) with values of $\beta > -1.5$. This may be useful for those planning further stacking analyses as the CDF-N survey is extended to 2 Ms.

Acknowledgments. This research has made use of the NASA/IPAC Extragalactic Database (NED) which is operated by the Jet Propulsion Laboratory, California Institute of Technology, under contract with the National Aero-

nautics and Space Administration. This work is supported by the NASA ADP program under the grants NAG5-8279 and NAG5-6400.

REFERENCES

- Adelberger, K. L. & Steidel, C. C. 2000, *ApJ*, 544, 218
 Arnaud, K. A. 1996, in ASP Conf. Ser. 101: Astronomical Data Analysis Software and Systems V, 5, 17
 Blain, A. W., Smail, I., Ivison, R. J., Kneib, J.-P., & Frayer, D. T. 2002, in *Physics Reports*, in press, (astro-ph/0202228)
 Brandt, W. N., Hornschemeier, A. E., Schneider, D. P., Alexander, D. M., Bauer, F. E., Garmire, G. P., & Vignali, C. 2001, *ApJ*, 558, L5
 Brandt, W. N. et al. 2001b, *AJ*, 122, 2810.
 Calzetti, D. 1997, *AJ*, 113, 162
 Calzetti, D., Armus, L., Bohlin, R. C., Kinney, A. L., Koornneef, J., & Storchi-Bergmann, T. 2000, *ApJ*, 533, 682
 Chapman, S. C. et al. 2000, *MNRAS*, 319, 318
 Cohen, J. G., Hogg, D. W., Blandford, R., Cowie, L. L., Hu, E., Songaila, A., Shopbell, P., & Richberg, K. 2000, *ApJ*, 538, 29
 Colbert, E. J. M. & Mushotzky, R. F. 1999, *ApJ*, 519, 89
 Dawson, S., Stern, D., Bunker, A. J., Spinrad, H., & Dey, A. 2001, *AJ*, 122, 598.
 David, L. P., Jones, C., & Forman, W. 1992, *ApJ*, 388, 82
 Draine, B. T. & Lee, H. M. 1984, *ApJ*, 285, 89
 Green, P. J., Anderson, S. F., & Ward, M. J. 1992, *MNRAS*, 254, 30
 Goldader, J. D., Meurer, G. R., Heckman, T. M., Seibert, M., Sanders, D. B., Calzetti, D., & Steidel, C. C. 2002, *ApJ*, in press
 Heckman, T. M., Robert, C., Leitherer, C., Garnett, D. R., & van der Rydt, F. 1998, *ApJ*, 503, 646
 Helou, G., Khan, I. R., Malek, L., & Boehmer, L. 1988, *ApJS*, 68, 151
 Hughes, D. H. et al. 1998, *Nature*, 394, 241
 Lanzetta, K. M., Yahata, N., Pascarelle, S., Chen, H., & Fernandez-Soto, A. 2002, *ApJ*, in press (astro-ph/0111129)
 Leitherer, C. et al. 1999, *ApJS*, 123, 3
 Madau, P., Ferguson, H. C., Dickinson, M. E., Giavalisco, M., Steidel, C. C., & Fruchter, A. 1996, *MNRAS*, 283, 1388
 Marcum, P. M. et al. 2001, *ApJS*, 132, 129
 Meurer, G. R., Heckman, T. M., Lehnert, M. D., Leitherer, C., & Lowenthal, J. 1997, *AJ*, 114, 54
 Meurer, G. R., Heckman, T. M., & Calzetti, D. 1999, *ApJ*, 521, 64 (MHC99)
 Morrison, R. & McCammon, D. 1983, *ApJ*, 270, 119
 Osterbrock, D. E. 1989, *Astrophysics of Gaseous Nebulae and Active Galactic Nuclei*, (Mill Valley: University Science Books)
 Papovich, C., Dickinson, M., & Ferguson, H. C. 2001, *ApJ*, 559, 620
 Persic, M. & Rephaeli, Y. 2002, *A&A*, 382, 843
 Pettini, M., Steidel, C. C., Adelberger, K. L., Dickinson, M., & Giavalisco, M. 2000, *ApJ*, 528, 96
 Rifatto, A., Longo, G., & Capaccioli, M. 1995, *A&AS*, 114, 527
 Roberts, T. P., Goad, M. R., Ward, M. J., Warwick, R. S., & Lira, P. 2002, in *New Visions of the X-ray Universe in the XMM-Newton and Chandra Era*, (The Netherlands: ESTEC), in press (astro-ph/0202017)
 Sandage, A. & Tammann, G. A. 1975, *ApJ*, 196, 313
 Sandage, A. & Tammann, G. A. 1981, *Revised Shapley-Ames Catalog of Bright Galaxies*, (Washington: Carnegie Inst. of Washington)
 Soifer, B. T., Sanders, D. B., Madore, B. F., Neugebauer, G., Danielson, G. E., Elias, J. H., Lonsdale, C. J., & Rice, W. L. 1987, *ApJ*, 320, 238
 Steidel, C. C., Adelberger, K. L., Giavalisco, M., Dickinson, M., & Pettini, M. 1999, *ApJ*, 519, 1
 Webb, T. M. A. et al. 2002, *ApJ*, in press (astro-ph/0201181)
 Williams, R. E. et al. 1996, *AJ*, 112, 1335
 Witt, A. N. & Gordon, K. D. 2000, *ApJ*, 528, 799

TABLE 1
 LYMAN-BREAK GALAXY SAMPLE

HDF ID	RA	DEC	z	$f_{8140, \text{obs}}$	$f_{1600, \text{rest}}$	β
(1)	(mm:ss.s)	(mm:ss.s)	(4)	(μJy)	(μJy)	(7)
4-858.0	36:41.25	12:03.1	3.220	867.04	757.84	-1.43
4-639.0	36:41.71	12:38.8	2.591	787.12	543.27	-0.76
2-82.1	36:44.07	14:09.9	2.267	459.37	481.26	-2.11
1-54.0	36:44.12	13:10.9	2.929	816.28	630.00	-0.96
4-445.0	36:44.64	12:27.4	2.500	1154.41	812.16	-0.81
4-316.0	36:45.09	12:50.8	2.801	811.71	729.93	-1.58
2-76.11	36:45.35	13:46.9	3.160	262.40	250.39	-1.90
4-289.0	36:46.95	12:26.1	2.969	296.98	311.44	-2.22
4-52.0	36:47.72	12:55.8	2.931	858.38	622.22	-0.70
2-449.0	36:48.34	14:16.6	2.005	1557.69	1056.20	-1.19
4-363.0	36:48.30	11:45.8	2.980	345.97	315.61	-1.65
3-243.0	36:49.81	12:48.8	3.233	264.29	228.68	-1.37
2-525.0	36:50.12	14:01.0	2.237	478.23	368.91	-1.48
2-565.1	36:51.19	13:48.8	3.162	186.71	162.94	-1.44
2-604.0	36:52.45	13:37.8	3.430	398.36	348.52	-1.31
2-637.0	36:52.76	13:39.1	3.369	341.51	312.94	-1.70
2-834.2	36:52.99	14:08.4	3.367	56.69	55.84	-2.19
2-591.2	36:53.18	13:22.8	2.489	385.16	324.58	-1.60
2-643.0	36:53.42	13:29.5	2.991	514.42	433.17	-1.30
2-901.0	36:53.60	14:10.2	3.181	522.11	440.26	-1.24
2-824.0	36:54.63	13:41.4	2.419	278.61	281.95	-2.06
2-903.0	36:55.08	13:47.0	2.233	541.35	496.64	-1.88
3-875.0	37:00.13	12:25.2	2.050	1079.74	825.69	-1.58
4-491.1	36:43.25	12:38.9	2.442	302.22	294.43	-1.99

Note. — (1) ID refers to HDF-N (V2) catalog of Williams et al. (1996). (2) RA (J2000) plus 12 hours. (3) DEC (J2000) plus +62 degrees. (4) Redshifts from Cohen et al. (2000) and Dawson et al. (2001). (5) Observed 8140Å flux density from catalog of Williams et al. (1996). (6) Interpolated 1600Å rest-frame flux density. (7) Photometrically derived UV spectral slope.